Scientific Reports

https://doi.org/10.1038/s41598-026-40041-4

Article in Press

Local heating induces an increase in the pulse wave velocity in peripheral vessels

Received: 6 November 2025

Accepted: 10 February 2026

Published online: 13 February 2026

Cite this article as: Kamshilin A.A., Podolyan N.P., Mizeva I.A. *et al.* Local heating induces an increase in the pulse wave velocity in peripheral vessels. *Sci Rep* (2026). https://doi.org/10.1038/s41598-026-40041-4

Alexei A. Kamshilin, Natalia P. Podolyan, Irina A. Mizeva, Oleg V. Mamontov, Valeriy V. Zaytsev, Maria E. Vasilieva, Victor A. Kashchenko, Anastasiia V. Sakovskaia, Polina M. Dolotovskaya, Nikita B. Margaryants & Roman V. Romashko

Local Heating Induces an Increase in the Pulse Wave Velocity in Peripheral Vessels

Alexei A. Kamshilin[1,], Natalia P. Podolyan[1], Irina A. Mizeva[2], Oleg V. Mamontov[3,4], Valeriy V. Zaytsev[1], Maria E. Vasilieva[5], Victor A. Kashchenko[5,6,7], Anastasiia V. Sakovskaia[8], Polina M. Dolotovskaya[1,9], Nikita B. Margaryants[10] and Roman V. Romashko[1]*

[1] Institute of Automation and Control Processes, Far Eastern Branch of the Russian Academy of Sciences, Vladivostok 690041, Russia

[2] Institute of Continuous Media Mechanics of Ural Branch of the Russian Academy of Sciences, Perm 614013, Russia

[3] Department of Circulation Physiology, Almazov National Medical Research Centre, Saint Petersburg 197341, Russia

[4] Department of Departmental Therapy, Pavlov First Saint Petersburg State Medical University, St. Petersburg 197022, Russia

[5] North-Western District Scientific and Clinical Center Named After L.G. Sokolov, FMBA, Saint Petersburg 194291, Russia

[6] Department of Faculty Surgery, St. Petersburg State University, Saint Petersburg 199106, Russia

[7] Beloostrov Clinic, Vsevolozhsk District, Leningrad Region 188651, Russia

[8] Institute of Therapy and Instrumental Diagnostics, Pacific State Medical University, Vladivostok 690990, Russia

[9] N.P. Bechtereva Institute of the Human Brain, Russian Academy of Sciences, Saint-Petersburg 197022, Russia

[10] Physical-Technical Megafaculty, ITMO University, Saint Petersburg 197101, Russian

*Corresponding author:

E-mail: alexei.kamshilin@yandex.ru (AAK)

Abstract

Accurate assessment of peripheral microcirculation is of great importance for wide range of clinical applications, from routine clinical examinations to patient monitoring in the operation room. Promising approach for assessing microcirculatory hemodynamics *in-vivo* is the use of a multimodal system based on synchronized imaging photoplethysmography (iPPG) and electrocardiography (ECG). However, precise estimation of the temporal characteristics of peripheral pulse waves is still a challenging task due to motion artifacts. In this study, we implemented data processing algorithm characterized by an increased signal-to-noise ratio. We analyzed 67 recordings of the microcirculation response in the forearm to local heating measured by the iPPG-ECG system from 47 healthy volunteers. A significant decrease in the pulse arrival time, accompanied by a multiple (up to 23-fold) increase in the pulsation amplitude was observed in all recordings after heating the forearm skin up to 41 °C. For the first time, an increase in the pulse wave velocity in a local peripheral area was detected. We interpret these findings as a consequence of an increase in the lumen of arteriovenous anastomoses in response to local heating. Therefore, the velocity of propagation of the arterial pulse wave is changed not only due to variations in the stiffness of the arterial walls but also because of redistribution of blood flow in the periphery, which is accomplished through the functioning of arteriovenous anastomoses. The advanced multimodal iPPG-ECG technique holds good promise for further in-depth studies of regional and central hemodynamics both in normal and pathological conditions.

Keywords. Arteriovenous anastomoses, imaging photoplethysmography, local heating test, microcirculation, pulse wave velocity, thermoregulation.

Introduction

The assessment of peripheral hemodynamics is of great practical importance both for evaluating the prognosis and course of peripheral trophic disorders[1] and for studying the mechanisms of systemic vascular regulation.[2] Based on the characteristics and reactivity of the cutaneous blood flow, a number of diseases can be diagnosed and their progression monitored. Methods for assessing peripheral blood flow are also relevant in cases of traumatic injuries,[3] endocrine and rheumatological diseases,[4,5] vascular pathologies[6] and disorders of the nervous system.[7]

Peripheral blood flow parameters can be assessed by a number of methods based on various physical principles. For this purpose, laser speckle contrast imaging, video capillaroscopy, near-infrared spectrometry, thermography, and laser Doppler flowmetry are used.[8,9] Imaging photoplethysmography (iPPG) is a promising technique, which allows contactless assessment of blood flow dynamics simultaneously in a wide field of view in both experimental and clinical settings.[10,11] The most accurate measurements of peripheral blood flow are provided by a multimodal system, which combines iPPG and electrocardiographic (ECG) techniques. This system is capable to evaluate both the amplitude and temporal (or phase) characteristics of the pulse wave.[12] One of the temporal parameters is a pulse arrival time (PAT), which is estimated as the delay time of the pulse wave arrival at the iPPG assessment point compared to the ECG R-peak.[13] Since the distance from the heart to the assessment point can also be estimated, PAT allows the pulse wave velocity (PWV) to be calculated. Its magnitude depends on the structure of the vascular bed, the diameter of the vessels, the stiffness of the vascular wall, pressure, and heart rate (HR).[14] Therefore, PWV can be used as a marker of arterial vascular stiffness and tone,[15,16] parameters that allow predicting the long-term outcomes

of patients with cardiovascular disease.[17] In addition, measuring the temporal parameters of the pulse wave is used as a basis for non-invasive monitoring beat-to-beat changes in blood pressure[18] and is attractive from the point of view of diagnosing vascular disorders and evaluating the effectiveness of therapy.[19]

However, not much is known about the factors influencing the pulse wave propagation in various parts of the vascular system. Most of the available methods allow evaluating the velocity of the pulse wave in large and medium-sized arteries, whereas the factors affecting the pulse wave propagation in microcirculatory vessels have not been sufficiently studied. Meanwhile, the local thermal impact is known to seriously affect microcirculation leading to a redistribution of skin blood flow in favor of the superficial capillary network.[20,21] Studying the local response of blood flow to moderate heating of the skin provides valuable information about the mechanism of local thermoregulation.

Our previous studies were devoted to assessment of amplitude parameters of the cutaneous blood flow in response to a heat impact.[22–24] In the current study, we perform an in-depth analysis of the experimental data obtained by our team in previous researches of the response of peripheral microcirculation to local heating in patients with risk factors for cardiovascular complications[23] and people with morbid obesity.[24] Given the obvious difference in these diseases, in this work we analyze only the data obtained for the control groups of these studies. This analysis was carried out using an advanced algorithm for processing the synchronously recorded iPPG and ECG data. The purpose of this study was to answer the question of whether PAT (and, consequently, PWV) undergoes significant changes in response to local skin heating of the forearm up to 41 °C.

Materials and Methods

Subjects

The study is based on 67 recordings of the reaction of blood flow parameters to local heating of the forearm in 47 healthy volunteers. Of these, 17 subjects underwent two or more repeated studies with an interval of several months between them. The anthropometric characteristics of the study participants are summarized in Table 1.

Table 1. Anthropometric data of the subjects selected for the study

Parameter	
Experimental sessions	n = 67
Subjects (male/female)	47 (31/16)
Age (years old)	37 ± 12
Body mass index (kg/m^2)	25 ± 4
Systolic blood pressure (mmHg)	119 ± 7
Diastolic blood pressure (mmHg)	77 ± 7

The study was carried out in the Institute of Automation and Control Processes of Far Eastern Branch of the Russian Academy of Sciences (Vladivostok, Russia), in the Private healthcare institution “Central clinical hospital “RZD-Medicine” Vladivostok”, and in the North-Western District Scientific and Clinical Center named after L.G. Sokolov (Saint-Petersburg, Russia). The investigations in all three institutions were conducted in accordance with the ethical principles of the Declaration of Helsinki (2013). The study protocols were approved by the Interdisciplinary Ethics Committee of the

Pacific State Medical University, Vladivostok, Russia (Protocol No. 10 of June 20, 2021) and by the Local Ethic Committee of the North-Western District Scientific and Clinical Center named after L. G. Sokolov (Protocol No. 3 of March 13, 2023). All participants provided written informed consent to participate in the study.

Study protocol

Measurement sessions were carried out in specially prepared darkened rooms with appropriate sanitary conditions at a temperature of 23 ± 1 °C. Prior the local heating test, subjects acclimatized to laboratory conditions for at least 15 minutes. Participants were instructed to refrain from taking caffeinated foods and any medications that could affect the cardiovascular function. The study protocols were virtually identical in all three centers, and have been described in detail previously.[23,24] Briefly, they consisted of three stages: (i) basal recording lasting 1 or 5 minutes, (ii) heating the skin up to 40 – 41 °C followed by maintaining the temperature for 15 – 20 minutes, and (iii) the recovery phase after the heater was turned off. The baseline duration was chosen to ensure sufficient data for assessment of iPPG parameters. The target heating temperature was chosen to induce maximal hyperperfusion, while the duration of heating should cover two main physiological vasodilation responses, axon reflex and humoral reaction.[21]

Measuring system

The layout of the experimental setup is shown in Fig. 1. Detailed description of all component of the multimodal system has been published

previously.[22] During the study, the subject was positioned comfortably either lying on his back or sitting in an armchair. The distal part of the forearm of the right hand was selected as a measurement site. A transparent glass plate (size of 2 × 7 cm^2) with an electrically conductive layer was used to heat the skin area.[22] The current supplied to the heater was regulated by a temperature controller connected with the laptop. A temperature sensor was installed between the plate and the skin to ensure continuous temperature monitoring. The thermal contact of the heater and the skin was provided with petroleum jelly. The pressure of the heater on the forearm did not exceed 15 mmHg for all subjects.

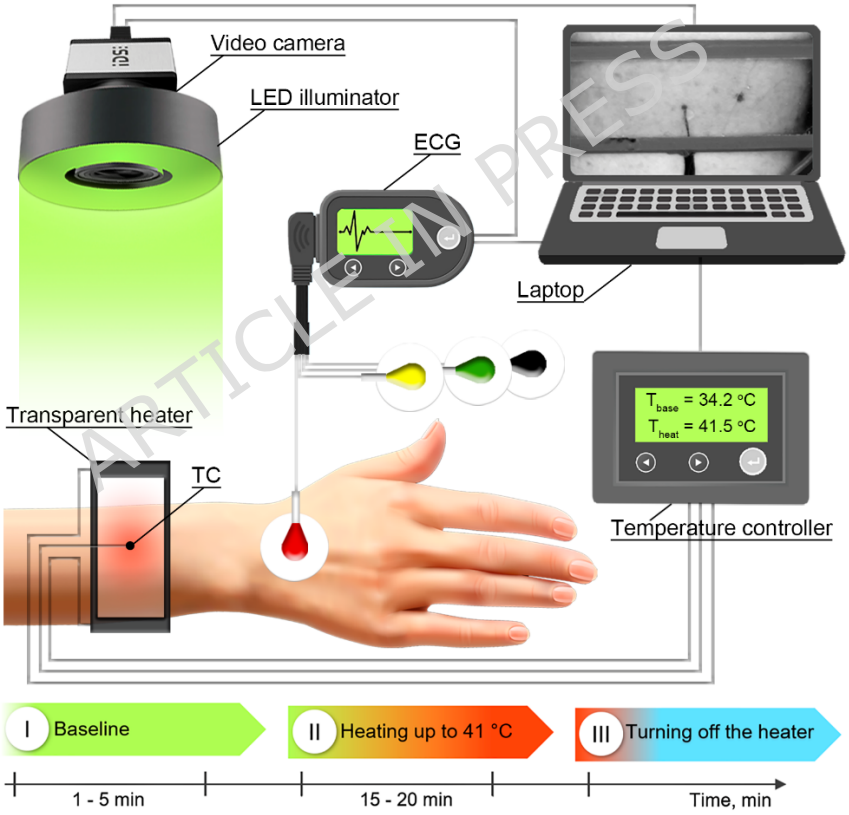

Fig. 1. Layout of the multimodal measurement system providing synchronous recording of an electrocardiogram (ECG) and images of forearm. Area under study is illuminated by green light-emitting diodes (LEDs). The local temperature is monitored by a temperature sensor (TS). Image frames are digitalized in a laptop, while ECG data and sync pulses from the camera are

digitalized in the ECG module to provide system's synchronization. A timeline of the experimental recording is shown in the lower part of the figure.

Changes in microcirculation parameters in response to a local heating were assessed using two multimodal iPPG-ECG systems, located in Vladivostok and St. Petersburg. Although both systems have a similar architecture consisting of a lighting module, a video camera, and an ECG module, their specific implementations differ. In Vladivostok, the lighting module contains 250 light-emitting diodes (LEDs) arranged in four concentric rings around the camera lens.[22,23] In St. Petersburg employs eight high-power LEDs (5 W each), similarly assembled around the camera lens.[24] In both systems, the LEDs were generating green light at a wavelength of 535 (halfwidth 25) nm. The choice of this wavelength was justified by the fact that the highest signal-to-noise ratio (SNR) in photoplethysmographic (PPG) measurements is observed when the skin illuminated with the green light.[25] Both systems used cameras of the same model: a monochrome 8-bit digital camera UI-3060CP-M−GL (Imaging Development Systems GmbH, Obersulm, Germany). In Vladivostok, the images were recorded at 36 frames per second (fps) with a resolution of 376 × 256 pixels, while in St. Petersburg it was done at 39 fps with a resolution of 752 × 480 pixels. Both systems used the same model of digital electrocardiograph (Kardiotechnika-EKG-8, Incart Ltd., St. Petersburg, Russia) to record a standard two-lead ECG with electrodes mounted on upper extremities. The ECG module incorporated an analog–digital converter with a sampling rate of 1 kHz. One channel of this converter continuously received synchronization pulses generated by the camera at the beginning of each frame. These pulses were digitized in parallel with the signals from standard ECG leads. By this way, the synchronization accuracy of 1 ms was achieved.[22] The ECG module transfers the data to the personal computer via the USB 3.0 port.

Data processing

The recorded data was processed by using custom software developed on the MATLAB® platform (version R2021a, The MathWorks, USA). Here we used a modified version of the algorithm described in our previous papers on local heating test data processing.[23,24] The goal was to increase the SNR. A central challenge in iPPG is its sensitivity to inevitable subject motion during *in-vivo* measurements.[26,27] Since both the skin and the capillary network are highly heterogeneous, even a slight displacement relative to the light source can lead to a significant change in the intensity of the reflected light than the desired modulation due to the pulse wave of blood pressure.

At the first stage, our algorithm applies digital stabilization of forearm images to minimize the influence of motion artifacts. Given that different parts of the image shift stochastically and in different directions, each frame was divided into 16 × 16 pixels segments, and the motion of each segment was compensated independently. We assume that there are two main reasons for the light intensity modulation: changes in blood volume interacting with light and tissue movement. The motion-related component is proportional to the image gradient and lateral offset. This component is evaluated in every segment of the frame by an optical flow algorithm using the gradient method.[28] After reconstruction, the motion-related component is subtracted from the original signal. Unlike previous versions of our algorithm, in which image offsets were estimated relative to the frame, which is the first in the whole recordings, here we calculated the intensity gradients for each cardiac cycle taken separately to increase the reliability of motion estimate. At the same time, the intensity gradient vectors were evaluated between two consecutive frames, since tissue displacement is minimal between consecutive frames. Gradients were

evaluated relative to the frame coinciding in time with the R-peak of the ECG signal of the cardiac cycle under consideration. Therefore, the images were stabilized separately for each cardiac cycle relative to the first frame in the cycle under assessment.

Second stage involves assessing spatial distribution of the pulse wave amplitude under two different physiological conditions, each time during a single cardiac cycle. One cycle was chosen in the initial (baseline) conditions, when the heater was turned off, while the other representative cycle was taken in the vasodilation state, four minutes after the heater was turned on. For hemodynamics mapping, the image was divided into small non-overlapping regions of interest (ROI) sizing 2 × 2 pixels, which is about 40 × 40 μm^2 in the forearm plane. A PPG waveform was calculated as frame-by-frame evolution of the average pixel value in each small ROI.

An example of the dynamics of the average pixel value during one cardiac cycle at baseline conditions is shown in Fig. 2A. The red curve shows the evolution of the mean pixel value in a small ROI assessed from a series of raw images. The magenta curve in Fig. 2A depicts the dynamics of the pixel value in the same ROI after image stabilization, implemented at the first stage of the algorithm. While the raw signal (red curve) exhibits high noise level, image stabilization significantly attenuates motion artifacts components. The remaining high-frequency component of the signal was suppressed by applying an infinite impulse response low-pass filter (9 Hz cut-off frequency) of the 12-th order, implemented using the MATLAB® filtfilt zero-phase function. The filtered evolution of the average pixel value in the small ROI is shown by the blue curve in Fig. 2A. This signal consists of an alternating component (AC) modulated at HR and a slowly varying component (DC). Light intensity

modulation at HR is associated with the arrival of a pulse wave to the periphery, whereas changes in DC during one cardiac cycle are related to muscles activity or changes in lymphatic pressure that may affect the compression of the capillary bed, as well. To diminish the impact of these factors, we removed the trend in DC by applying the following equation:

$$I^{dt}_{ROI}(t) = \frac{I^{flt}_{ROI}(t_{R2}) - I^{flt}_{ROI}(t_{R1})}{t_{R2} - t_{R1}} - I^{flt}_{ROI}(t). \quad (1)$$

Here $I^{dt}_{ROI}(t)$ and $I^{flt}_{ROI}(t)$ are evolutions of the mean pixel value in the ROI during one cardiac cycle for differential and filtered signal, respectively; t_{R1} and t_{R2} are the time of occurrence of the initial and final R-peak for a given cardiac cycle, respectively. The terms $I^{flt}_{ROI}(t_{R1})$ and $I^{flt}_{ROI}(t_{R2})$ correspond to magnitudes of the filtered signal at time t_{R1} and t_{R2}, respectively. The negative sign in (Eq. 1) before $I^{flt}_{ROI}(t)$ ensures that the PPG signal is inverted so that changes in the waveform are positively correlated with changes in blood pressure.[29] The linear trend is shown by the dashed green line in Fig. 2A.

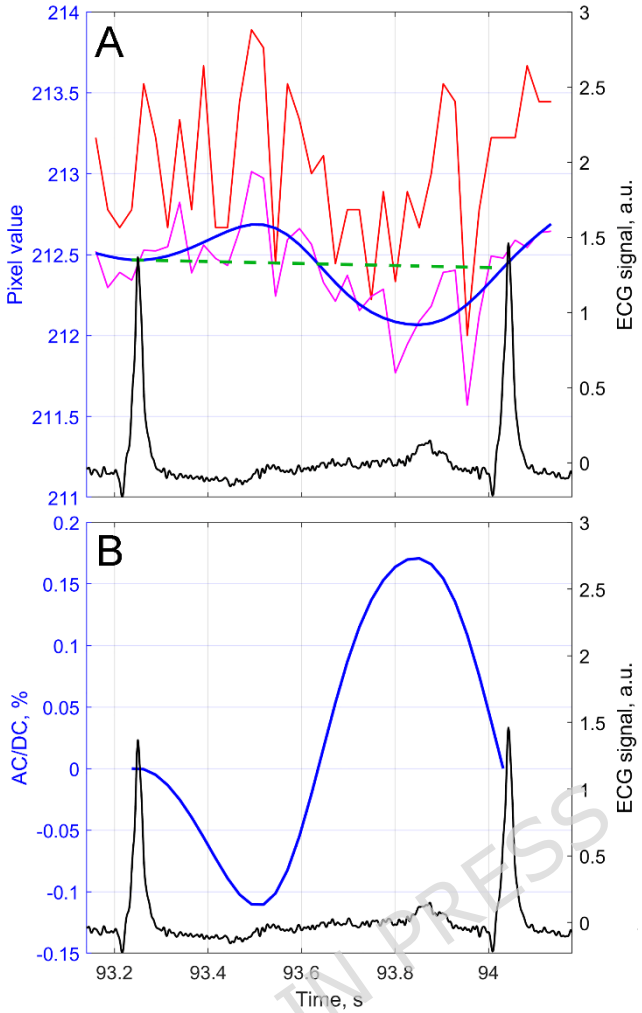

Fig. 2. An example of processing the average pixel value in a small ROI for one cardiac cycle. (A) The red curve shows the dynamics of the average pixel value estimated from a series of raw images. The magenta curve shows the mean pixel intensity dynamics after digital stabilization. The blue curve shows the signal after stabilization and high-frequency filtering. The dashed green line indicates the linear trend of the pixel value during the cardiac cycle. (B) The resulting waveform $\mathrm{PPG}_{\mathrm{norm}}$ is shown by the blue line after inverting, detrending and normalizing the filtered signal. In both panels, the black line shows the ECG signal, which defines the position in time of the cardiac cycle.

To compensate for uneven illumination, we normalized the differential filtered signal to the mean DC value as

$$\mathrm{PPG}_{\mathrm{norm}} = \frac{I^{dt}_{ROI}(t)}{I^{flt}_{ROI}(t_{R2}) + I^{flt}_{ROI}(t_{R1})} 200\%. \quad (2)$$

The resulting normalized waveform $\mathrm{PPG}_{\mathrm{norm}}$ is shown by the blue curve in Fig. 2B and hereinafter referred to as the PPG waveform. This waveform

exhibits the classical shape of a photoplethysmographic signal, demonstrating the efficacy of the proposed algorithm for increasing the SNR. The PPG waveform is used to estimate the blood flow parameters: an amplitude of the pulsatile component (APC) determined as the difference between the maximum and minimum of PPG_{norm}, and PAT defined as the time difference between the ECG R-peak and the subsequent minimum of PPG_{norm}. Both the parameters were calculated for every cardiac cycle in each small ROI.

The third stage of the algorithm involves the quantitative assessment of the blood flow dynamics in response to local heating. Using the APC map calculated at the previous stage for the vasodilation state, we choose two large circular ROIs with a radius of 21 pixels. Averaging over such a larger number of pixels allowed us to obtain a PPG waveform with higher SNR. One ROI was set inside the heating region, while the other was placed outside it. The location of these large ROIs was chosen in such a way as to avoid the presence of skin damage or scars inside. ROI in the area of contact of the heater with the skin was selected in places with elevated APC values. For each of the large ROIs, the normalized PPG waveform (Eq. 2) for every cardiac cycle from the beginning to the 15th minute of each recording was calculated. The APC and PAT parameters were assessed from the PPG waveform in each cardiac cycle similarly we did it for small ROIs. A detail description of the APC and PAT calculation procedure is provided in the Section III.

Statistical analysis

The samples obtained in the experiment were tested for compliance with the Gaussian distribution using the Shapiro-Wilk test. For non-Gaussian distributions, the results are presented as Me [Q1-Q3], where Me represents

the median value of the sample, Q1 and Q3 are the first and the third quartiles of the distribution, respectively. In the case of Gaussian distributions, the results are presented as the mean ± standard deviation. The significance of differences between averages of related samples is determined using the Wilcoxon criterion. The differences are accepted as significant at the level of statistical significance $P < 0.05$.

Results

Spatial distribution of microvascular responses to heating

Figure 3 presents examples of grayscale raw images of the forearm area under study taken at the baseline (Fig. 3A) and four minutes after turning on the heater (Fig. 3D). During the baseline period, illumination of the forearm is fairly uniform (Fig. 3A). However, after heating, the region under the heat source within the boundaries of the heat-conducting lubricant becomes darker. It is worth noting that the increase in green light absorption in the heated area does not exceed 20% of the initial level of the returned light intensity for all subjects. APC mappings overlaid with the initial images before and after heating are shown in Fig. 3B and 3E, respectively.

In the particular example shown in Fig. 3B, the APC before heating is evenly distributed over the area under study in the range from 0.15 to 0.30 %. When the skin temperature exceeds 40 °C (Fig. 3E), a multiple increase in the APC is observed near the center of the heated zone. It is worth noting that in most of the subjects, the increase in the APC outside the heated zone was much less than that directly under the heater, as shown in Fig. 3E. A similar pattern

of changes in the spatial distribution of APC due to local heating was revealed in all 67 recordings.

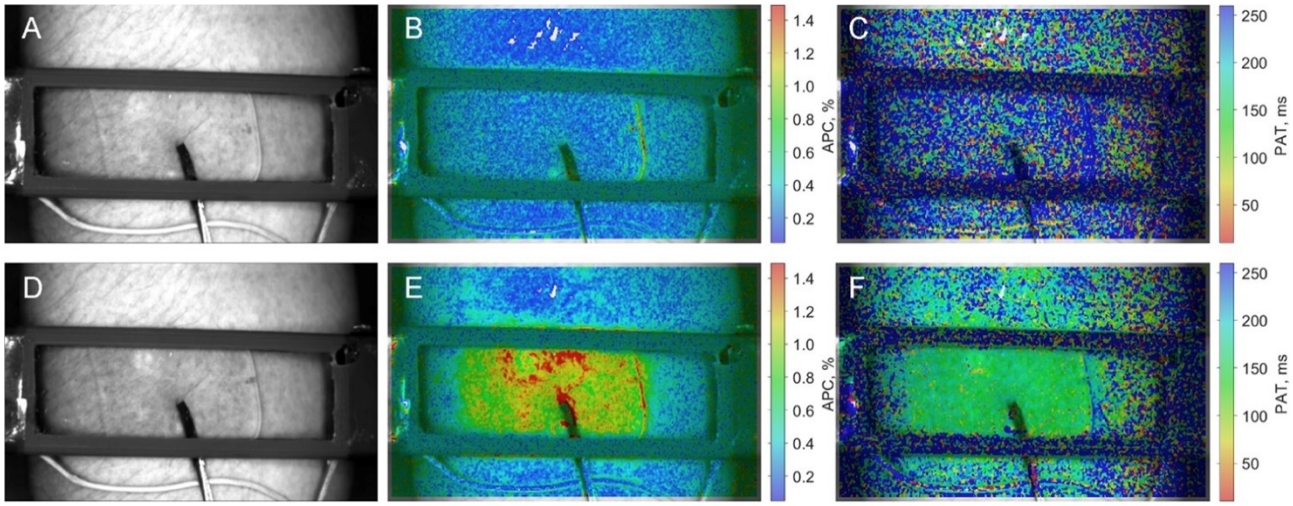

Fig. 3. Raw images of the area under study and spatial distributions of the amplitude of the pulsatile component (APC) of the photoplethysmographic waveform and the pulse arrival time (PAT) in this area, obtained under initial conditions (upper row: A, B, C) and after skin heating to 41 °C (lower row: D, E, F). Grayscale images of the forearm area with the heater (black frame) illuminated by green light are shown on panels A and D. The APC and the PAT maps were assessed for the same cardiac cycle during baseline (panels B and C, respectively) and during another cycle after heating (panels E and F, respectively). All mappings are displayed in pseudo colors with respective color scales on the right.

Figure 3C shows the spatial distribution of PAT assessed under baseline conditions, which exhibits a relatively random pattern. This variability arises because both PAT and APC mappings were assessed using small ROIs of 2×2 pixels during a single cardiac cycle, and thus they are affected by noise. Nevertheless, we demonstrate them for a qualitative, visual assessment of the heating impact. Referring to the color bar in Fig. 3C, it can be estimated that PAT before heating varies from 0.15 to 0.25 seconds. An increase in skin temperature causes PAT in the area of contact with heater to decrease to 0.13 – 0.14 seconds. As shown in Fig. 3F, such a reduced magnitude of PAT is evenly distributed within the entire contact area. It should be emphasized that a

uniform distribution of PAT over the area of skin contact with the heater was observed in all subjects.

Responses inside and outside the heated area

Based on the calculated spatial distributions of the APC under heating conditions (such as shown in Fig. 3E), two ROIs for each subject were selected. One ROI was located in the area of the most pronounced increase in APC within the region of skin contact with the heater, while the other was placed outside the heater to compare the hemodynamic responses on the external heating inside versus outside the zone of contact the heater with the skin. Figure 4 shows one more example of the APC spatial distribution of before (Fig. 4A) and during (Fig. 4B) local heating, obtained from another subject. Positions of the selected ROIs are shown by red and blue circles for inside and outside regions, respectively.

By comparing the APC mappings when the skin is heated (Fig. 3E vs Fig. 4B), it is evident that both subjects exhibit a pronounced increase in APC just in the area bounded by the heat-conducting lubricant that ensures thermal contact of the heater with the skin. A similar spatial distribution, characterized by a stronger increase in APC inside the contact zone of the heater with the skin, was observed in all subjects without exception. This finding emphasizes the important role of using heat-conductive lubricant in our experiments. Nevertheless, the comparison of the APC mappings in Fig. 3E and Fig. 4B reveals the variability in responses among different subjects. If in Fig. 3E, near the upper boundary of the heater, only a small increase in APC is visible outside the heater frame, then in Fig. 4B, the increase in APC outside the heater is much higher and extends over greater distances from the frame.

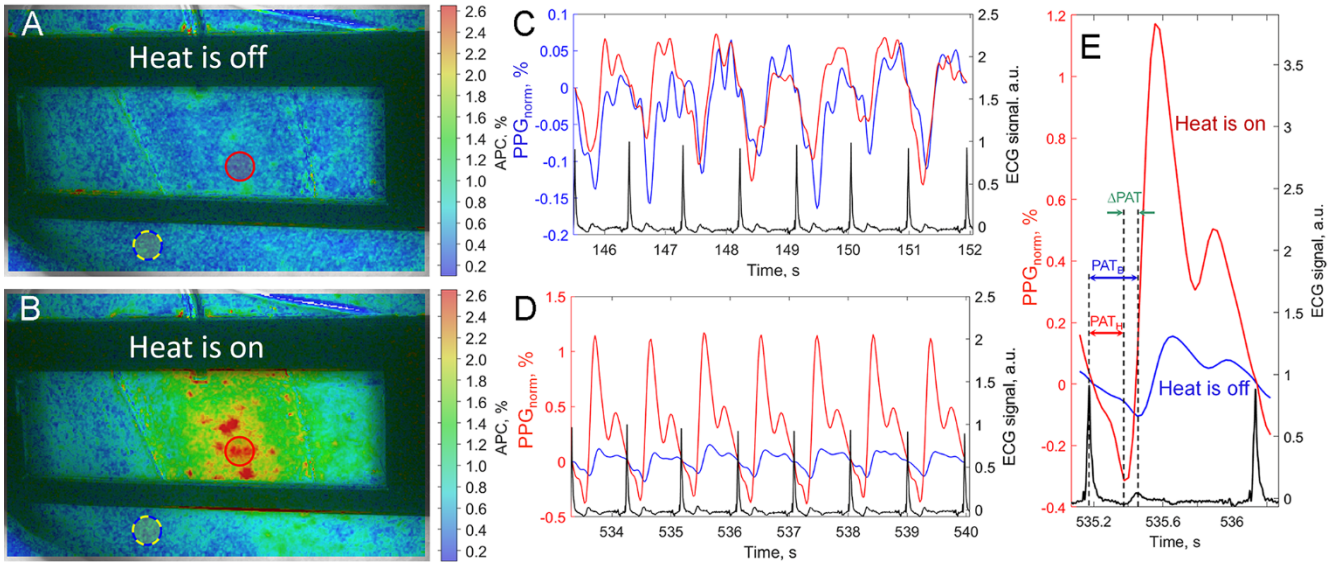

Fig. 4. Spatial and temporal characteristics of pulse waves. (A) An example of the spatial distribution of the amplitude of the pulsatile component (APC) of the photoplethysmographic waveform measured before heating at 2.5 minutes for one cardiac cycle. (B) APC distribution measured at the 9th minute (four minutes after turning on the heater). Red and blue circles in panels A and B indicate selected ROIs. (C) Photoplethysmographic (PPG) waveform averaged within the ROI selected in the area of skin contact with the heater (red line) and outside the heater (blue line) assessed during seven seconds in the baseline before the heating. (D) PPG waveform in the same ROIs but assessed 3.9 minutes after the heater was switched on. (E) Enlarged PPG waveforms with notations of the pulse arrival time (PAT) assessed in the ROIs inside and outside the heater for one cardiac cycle at the 9th minute. The black curves in panels C, D, and E show the synchronously recorded electrocardiogram (ECG).

It should also be noted that under the baseline conditions (prior to heating), APC outside the heated zone does not significantly differ from that within the contact zone for most of the subjects. This means that neither the lubricant nor the contact pressure of the heater significantly affects the basal blood flow in the area under study.

Typical PPG waveforms assessed in two ROIs located inside and outside the contact zone of the heater with the skin are shown in Fig. 4C (before heating) and 4D (after heating) for seven cardiac cycles. Red curves in these panels show the PPG waveforms inside the heater, while blue curves represent

the waveforms outside. In the baseline conditions (Fig. 4C), the waveforms inside and outside the heater are similar in shape. Since the AC/DC ratio is quite small (less than 0.1%) in the baseline conditions, noise can seriously affect the shape of the measured pulse wave. However, it is worth noting that in the baseline, the minima of the red (ROI inside the heater) and blue (ROI outside the heater) curves occur with almost the same delay relative to the R-peaks. Figure 4D shows that heating the skin leads to a significant increase in the modulation amplitude of the PPG waveform inside the heater (red curve), whereas the increase in the signal outside the heater (blue curve) is modest. At the same time, it is clear that the minima of the red curve in Fig. 4D are closer to the R-peaks of the ECG signal as compared to the minima of the blue curve. This means that the pulse wave reaches the forearm inside the heater earlier than it does outside.

PPG waveforms assessed after heating both inside and outside the heated zone during just one cardiac cycle are explicitly shown in Fig. 4E. In this particular case, the PAT measured within the contact zone of the heater with skin is 205 ms, which is significantly lower than 278 ms for the PAT assessed in the ROI outside the heater. Since the PAT inside and outside the heated zone did not differ statistically from each other at the baseline (see Fig. 4C), the difference between them actually corresponds to a decrease in the PAT inside the heating zone due to heating. Note that after heating, the PPG waveform takes on a classic shape with almost imperceptible noise influence.

Changes in APC and PAT due to heating

In all the subjects studied, local heating of the forearm led to a significant increase in the APC and a simultaneous decrease in the PAT. Typical responses of these parameters to heating are shown in Fig. 5, in which we selected just

six of the 67 recorded sessions to demonstrate the high variability in parameters of the blood flow in response to the local heating. While in some subjects, heating to 41 °C leads to a threefold increase in the APC (panel A), in others, this parameter increases by more than 20 times (panels C and F).

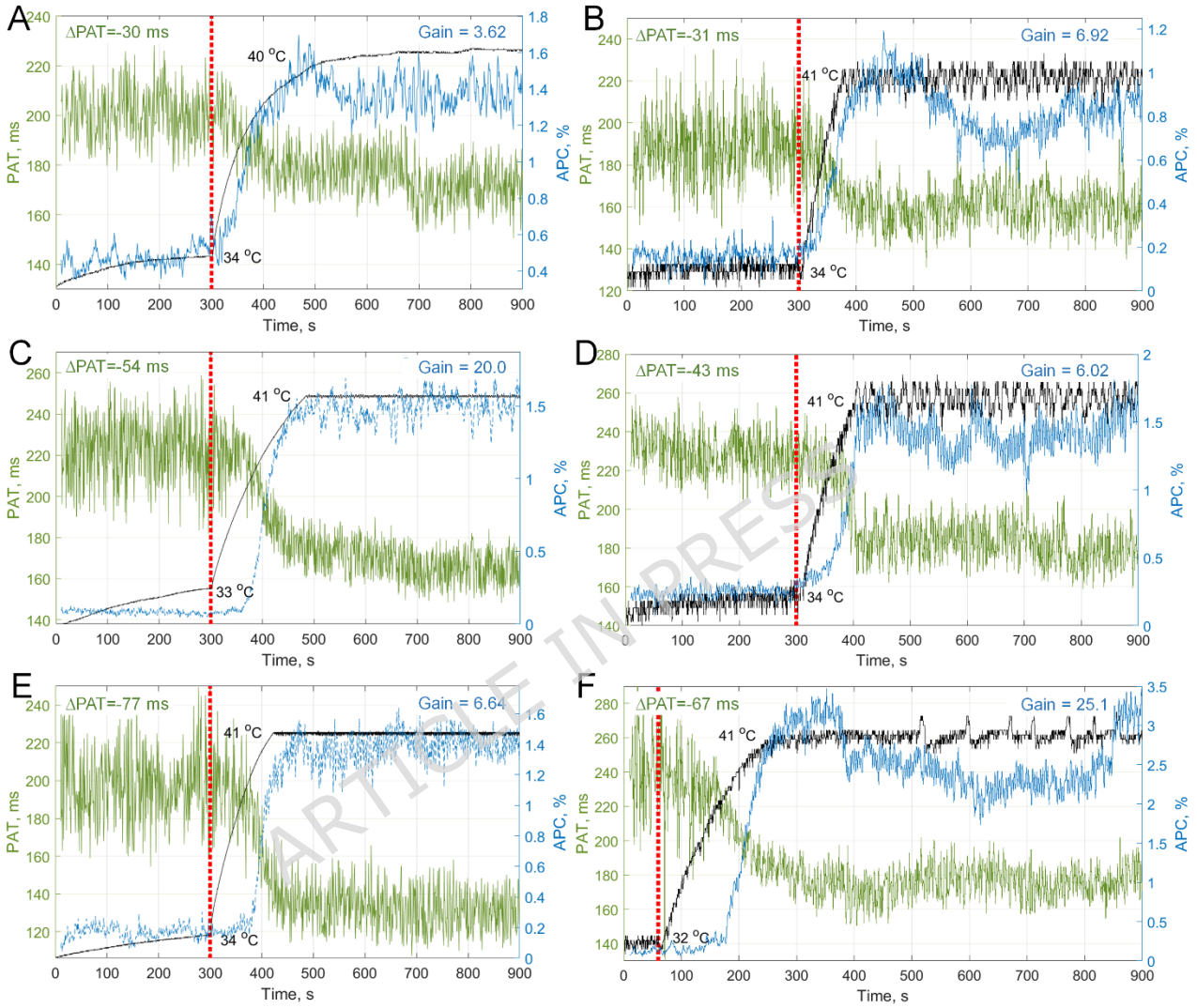

Fig. 5. Typical examples of the response of blood flow parameters to local heating of the forearm. Vertical red dotted lines in each panel indicate when the heater was turned on. Blue lines show changes in the amplitude of the pulsatile component (APC), while green lines refer to changes in the pulse arrival time (PAT). Changes in skin temperature in the area of contact with the heater are shown by black curves on all panels.

The change in the PAT parameter (ΔPAT) induced by heating considerably varies. For the recordings in panels A and B, it is about 30 ms, while for the subjects whose responses to heating are shown in panels E and F of Fig. 5, it

doubles to ΔPAT > 60 ms. It is worth noting that in all subjects whose reactions are shown in Fig. 5, the PAT is less than 180 ms after heating, and for the subject shown in panel E, it is 130 ms. Before heating, the PPG waveform is more susceptible to noise, resulting in a greater spread of the PAT data compared to measurements taken after heating.

Moreover, there is a significant variation in the delayed response to heating in different subjects: if on panels A, B, and D, changes in both APC and PAT practically follow an increase in skin temperature, then on panels C, E, and F, a response delay is clearly visible, reaching as much as 120 ms for the subject whose response shown in Fig. 5F. In any case, we must emphasize observation of a similar pattern for all subjects: heating leads to an increase in the APC, which is accompanied by a decrease in the arrival time of the pulse wave (PAT). For statistical analysis, we calculated the average values of both APC and PAT in the baseline and heating stages. To this end, in each of the sessions, we selected a sequence of 50 cardiac cycles, in which there were no outliers. The difference in the average PAT before and after heating is denoted by ΔPAT, and the ratio of the average APC in the heating stage to that in baseline is denoted as a gain.

Figure 6 shows the distribution of APC and PAT across all the recordings (n = 67). Under the baseline conditions, APC equals to 0.21 [0.16-0.31] %, and heating the skin to 41 °C leads to an increase in APC up to 1.55 [1.39-1.83] %, $P < 0.0001$ (see Fig. 6A). APC increases in 7.2 [5.4-10.4] times with a maximum and minimum gain 23.3 and 2.3, respectively (Fig. 6B). Here the gain is defined as the ratio of the APC value measured after heating to the value before heating. PAT under the baseline conditions is 222 [195-242] ms, decreasing to 169 [155-190] ms, $P < 0.0001$ (see Fig. 6C). Distribution of the difference in PAT over the

studied sample is shown in Fig. 6D: ΔPAT = 47 [38-61] with the minimum of 15 ms and the maximum of 111 ms.

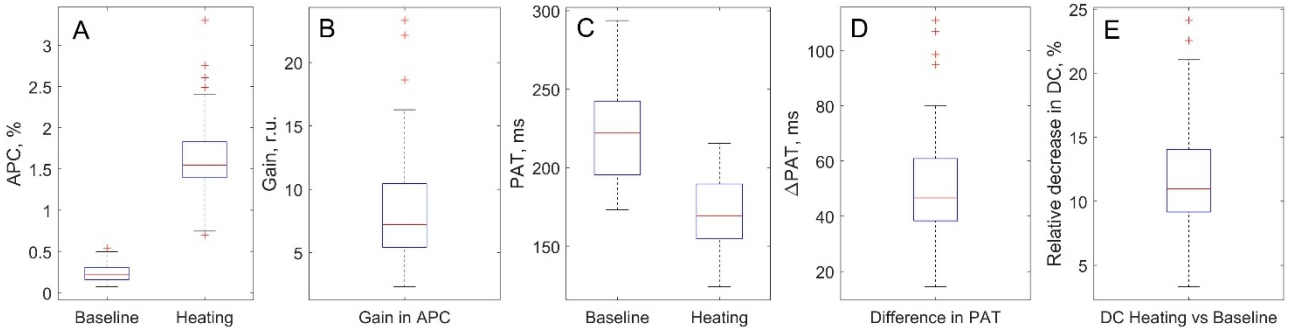

Fig. 6. Box-whisker diagrams of the amplitude of pulsatile component (APC) of the photoplethysmographic waveforms and pulse arrival time (PAT) in the sample under study. (A) APC before and after heating. (B) Gain in APC due to heating. (C) PAT before and after heating. (D) Difference in PAT (ΔPAT) caused by heating. (E) The relative decrease in the slowly varying component (DC) of the photoplethysmographic waveform assessed after heating compared to the baseline.

Moreover, our study has revealed that local heating leads to only a moderate change in the DC component of the iPPG waveform. The relative change of this component was assessed as the ratio of the difference between the heated and baseline values (measured in the same ROI), normalized to the baseline value and expressed as a percentage. It was found that the DC component in the baseline is always higher than in the heating state with the relative change of 10.9 [9.2 – 14.1] % (see Fig. 6E).

Discussion

The microcirculation response to local heating of the forearm has been thoroughly studied,[30–34] including fluctuations in blood flow of different frequencies responsible for various mechanisms of microcirculatory regulation.[35,36] Most researchers reported a multiple increase in perfusion of the forearm area with local heating of the skin.[32–34,36–38] The present study

analyzes changes in both phase and amplitude parameters of the blood pulse wave caused by a response to local heating. For this purpose, we used a multimodal system, which includes synchronized iPPG and ECG modules. This approach makes it possible to measure parameters of skin perfusion dynamics with high spatial and temporal resolution in a wide field of view.

Here, for the first time, we have demonstrated that local hyperemia leads to a significant (more than 30%) decrease in PAT. The decrease was observed in all recordings without a single exception. The observed decrease in PAT is undoubtedly local in nature, as evidenced by two observations. First, we did not find a statistically significant change in HR during the local hyperemia test. This means that systemic hemodynamics is not involved in the process associated with the response of blood flow to local heating. This observation is in agreement with the data of other authors who evaluated the ECG during local heating of the forearm.[39] Second, the detected changes in APC and PAT parameters are local in nature in the sense of spatial distribution over the skin: no changes in both parameters were observed either distal or proximal to the heater. This means that local heating does not change the basic mechanical properties of the walls of large arterial vessels.

Considering that the distance from the heart to the assessment point of the iPPG parameters remains unchanged during the local heating, the observed decrease in PAT should be interpreted as an increase in PWV. Since the large arterial vessels do not change their properties after local heating (see above), the change in PWV occurs at the level of microvessels. Let us estimate the difference in the arrival time of pulse waves to the red and blue ROIs, which are separated in space by two centimeters from each other (see Fig. 4B). Typical velocity of pulse waves in large vessels is about 8 m/s.[40] Thus, if we assume that

the difference in the arrival time of pulse waves occurs when they propagate through large vessels, then we obtain ΔPAT = 2.5 milliseconds, which is 20 times less than the difference observed in the study. The increase in PWV can only be explained by the decisive influence of the microcirculatory bed on the propagation velocity of the pulse wave.

With local heating, the mechanical properties of the microcirculatory bed undergo significant changes, which is confirmed by a multiple increase in APC. Let us consider two adjacent microcirculatory nodes, one of which is located inside the heated area, and the other outside, as shown schematically in Fig. 7. Each node consists of a feeding arteriole, capillaries, an arteriovenous anastomosis (AVA), and a venule. Arterioles are vessels whose hemodynamic resistance can vary widely with changes in their vascular tone. Heating causes a decrease in vascular tone, which leads to both an increase in the lumen of the arterioles and an increase of vascular compliance.[38] Blood from the arterioles enters the capillaries, which are vessels without a vascular wall in which metabolic processes between blood and tissue take place. Capillaries are the smallest vessels of the cardiovascular system. Previously, it was assumed that the flow through them is regulated by precapillary sphincters, but in modern studies this fact is doubtful.[41] In our optical measurements of the microcirculation response to local heating, we did not observe well-marked signs of "opening" and "closing" of precapillary sphincters, as well. Indeed, assuming that heating increases the number of functioning capillaries, one would expect that the observed multiple increase in the AC component of the PPG waveform is accompanied by a corresponding decrease in the DC component, since the increased number of RBCs in additionally open capillaries should absorb more light. However, our measurements clearly showed that the

average decrease in the DC component for the entire group is only 9.6%, while APC demonstrates a sevenfold increase in average (see Fig. 6). Therefore, we assume that local heating only slightly changes the hemodynamic resistance of the capillaries, since their number remains approximately equal to what it was before heating, and the lumen of the capillaries cannot change. In addition, since the circulatory system is closed, in order to explain the observed increase in PWV, we must assume the presence of additional pathways bypassing the capillary network, which significantly change their hydrodynamic resistance when heated. These are AVAs that can serve as such bypass routes.

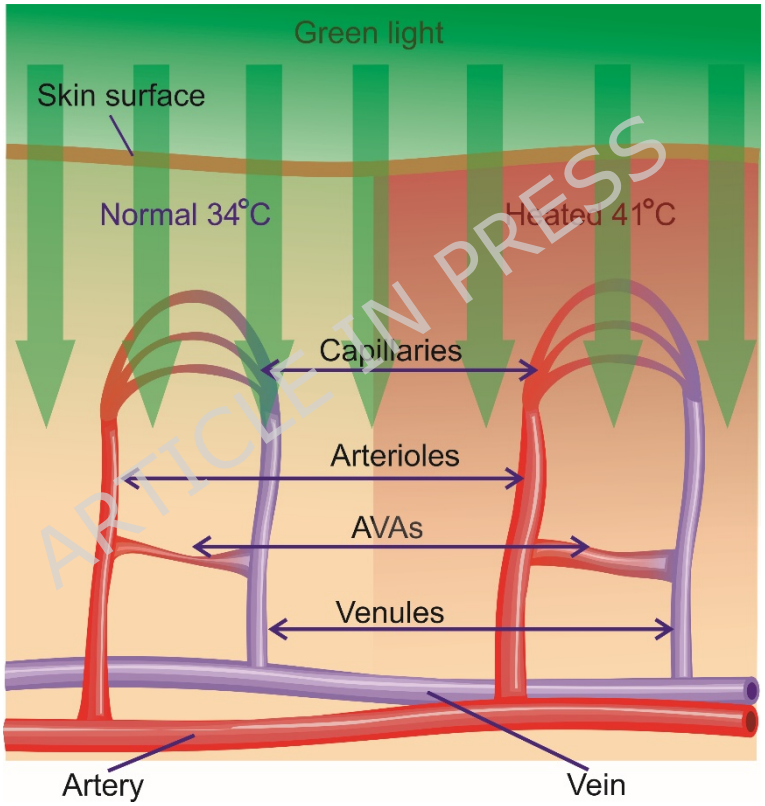

Fig. 7. Diagram of microcirculatory nodes and variations of their components under the influence of local heating. The microcirculation node consists of a feeding arteriole, an arteriovenous anastomosis (AVA), capillaries, and a venule.

These vessels, like arterioles, can change the lumen, which leads to the redirection of blood flow directly into the venules parallel to the capillary bed. AVAs, especially in their middle segment, differ significantly from the surrounding vessels by the presence of a rich innervation of an adrenergic

nature. This creates conditions for regulating the lumen of AVAs independently of other vessels, ensuring an operational redistribution of blood flow between the superficially and deeply located vessels of the skin.[42] They behave in much the same way as arteries and arterioles, but show much greater vasomotor activity.[42,43] Despite the long period of study, the number, shape, and spatial distribution of AVAs in various parts of the body remain a subject of discussion.[44] Many researchers are of the opinion that AVAs are mainly occur in glabrous (hair-free) skin, but absent in nonglabrous skin.[42–44] Recently, in an attempt to evaluate the effect of AVAs on microcirculation, Cao et al. reported the observation of statistically significant difference in the amplitude of the PPG waveform assessed simultaneously in areas of glabrous and nonglabrous skin.[45] The venous part of the microcirculatory bed has no significant effect on the detected effect of the increase in PWV.

We propose the following explanation for the observed increase in PWV due to local heating. The velocity of propagation of the pulse wave depends on the diameter of the vessel and its mechanical properties. It is known that heating causes a decrease in arteriole tone, resulting in dilation of the feeding arteriole and AVA.[21,38] This situation is schematically illustrated in Fig. 7, where the left microcirculatory node is in an undisturbed state, while the right one is heated. The penetration of light into tissues plays an important role in modeling the mechanism of signal formation. Since the greatest amplitude of the PPG-waveform modulation at HR is observed under green illumination,[46,47] this light was used in our iPPG system. The conventional model of PPG-signal formation suggests that the main reason for light intensity modulation is a change in blood volume in vessels due to their pulsatile nature.[48] However, the observed high modulation of green light is difficult to explain within the framework of this

model, since RBCs in the capillary layer efficiently absorb this light, which determines its small penetration depth (<0.5 mm)[49] and, accordingly, the low probability of its interaction with pulsatile vessels. It should also be taken into account that capillaries do not pulsate at HR because their average diameter is smaller than the mean size of RBCs and their walls are too rigid.[50,51] It is worth noting that green light can penetrate deeper in the classical reflection-type PPG technique, which uses spatially separated light source and detector in contact with the skin, ensuring the propagation of light in a so-called “banana-shaped” path.[52] However, banana-shaped light paths are unlikely to be occurred in the contactless iPPG. Therefore, we hypothesize that the leading role in the formation of the iPPG signal under green illumination is played by mechanical compression and relaxation of the intercapillary tissue by pulsating walls of more deeply situated arteries and arterioles.[25] A decrease in the tone of arterioles and AVAs of the heated microcirculatory node leads to an increase in the amplitude of oscillations of their walls at HR, which is the reason for the observed increase in APC.

It should be emphasized that an increase in the APC accompanied by a decrease in the PAT in response to local heating was observed in all subjects without exception (see Fig. 6). Nevertheless, the magnitude of the changes varies greatly from one subject to another. In addition to variations in the APC gain and ΔPAT among the subjects, there is also a large variability in the delay of the microcirculation responses to the onset of heating (see Fig. 5). We assume that these dissimilarities are caused by individual differences in processes of thermoregulation in which AVAs play an important role.

As we have already noted, iPPG provides measurements of blood flow parameters in contactless manner. This is essential to minimize the impact of

the measurement system on the circulatory system during *in-vivo* measurements. However, in order to ensure efficient heat transfer from the heater to the subcutaneous tissue, contact of the heating glass with the skin is necessary. Despite the fact that the contact area is large enough, while the pressure on the skin is small and controlled, such contact can affect the measured blood flow parameters, which represents a limitation of our study. To resolve this issue, our recent-future plan includes carrying out a study in which the tissue heating will be also non-contact. Nevertheless, the main conclusion about a significant decrease in the PAT with a simultaneous increase in the APC should be considered with a high degree of reliability, as it is unlikely that the invariable skin-heater contact pressure over time could affect the dynamics of changes in blood flow parameters.

Conclusions

In this study, we have demonstrated for the first time that an increase in skin temperature in the local region of the forearm leads to a decrease in pulse arrival time. This decrease is accompanied by well-known multiple increase in the amplitude of the pulse wave in the heated region. The locality of the observed changes in PAT and APC is validated by the apparent absence of significant changes in both heart rate and hemodynamic parameters in the vicinity of the heated area. We interpret the results obtained as a consequence of an increase in the lumen of arterioles and AVAs in response to heating of the region under study. Our experimental findings show that an increase in the velocity of the peripheral pulse wave occurs not only due to an increase in stiffness of the arterial walls but also as a consequence of the redistribution of blood flow through AVAs. The advanced multimodal iPPG-ECG technique is a

valuable tool that allows experimental assessment of the functioning of AVAs *in-vivo*, which is unlikely to be achieved by other methods. Such a system has good prospects for further in-depth study of regional and central hemodynamics in normal and pathology conditions.

Ethics statement

The investigations were performed in accordance with the ethical standards presented in the 2013 Declaration of Helsinki. The study plans were approved by the Interdisciplinary Ethics Committee of the Pacific State Medical University, Vladivostok, Russia (Protocol No. 10 of June 20, 2021) and by the Local Ethic Committee of the North-Western District Scientific and Clinical Center named after L. G. Sokolov (Protocol No. 3 of March 13, 2023). All the participants of the study signed a written informed consent form attached to the protocols of the relevant ethics committees.

Funding

This research was supported by funding from the Russian Science Foundation (Project No. 25-15-00400) in terms of software development and data processing and from the Ministry of Science and Higher Education of Russian Federation (Agreement No. 125020301282-0) in terms of manufacturing and calibration of the iPPG system.

Authors Contribution

A.A.K.: Writing – original draft, Writing – review & editing, Project administration, Data curation, Software, Methodology, Conceptualization. **N.P.P.:** Writing – review & editing, Investigation, Data curation, Visualization.

I.A.M.: Writing – original draft, Writing – review & editing, Data curation, Visualization. **O.V.M.:** Writing – review & editing, Formal analysis, Validation, Conceptualization. **V.V.Z.:** Software, Methodology, Resources. **M.E.V.:** Investigation, Methodology, Formal analysis. **V.A. K.:** Writing – review & editing, Project administration, Supervision. **A.V.S.:** Investigation, Methodology, Formal analysis. **P.M.D.:** Investigation, Data curation. **N.B.M.:** Data curation, Investigation, Writing – review & editing, Resources. **R.V.R.:** Supervision, Project administration, Funding acquisition.

Declaration of competing interest

The authors declare that they have no known competing financial interests or personal relationships that could have appeared to influence the work reported in this paper.

Availability of data and materials

The data obtained and analyzed during the current study are available from the corresponding author on reasonable request.

References

1. Steinmetz, O. K. & Cole, C. W. Noninvasive blood flow tests in vascular disease. *Can. Fam. Physician* **39**, 2405-2410,2413-2416 (1993).
2. Mamontov, O. V., Zaytsev, V. V. & Kamshilin, A. A. Plethysmographic assessment of vasomotor response in patients with congestive heart failure before and after heart transplantation. *Biomed. Opt. Express* **15**, 687–699 (2024).
3. Kamolz, L.-P., Andel, H., Auer, T., Meissl, G. & Frey, M. Evaluation of Skin Perfusion by Use of Indocyanine Green Video Angiography: Rational Design and Planning of Trauma Surgery. *J. Trauma Acute Care Surg.* **61**, 635–641 (2006).
4. Clarkson, P. *et al.* Impaired vascular reactivity in insulin-dependent

diabetes mellitus is related to disease duration and low density lipoprotein cholesterol levels. *J. Am. Coll. Cardiol.* **28**, 573–579 (1996).

5. Van Der Geest, K. S. M., Sandovici, M., Brouwer, E. & Mackie, S. L. Diagnostic Accuracy of Symptoms, Physical Signs, and Laboratory Tests for Giant Cell Arteritis: A Systematic Review and Meta-analysis. *JAMA Intern. Med.* **180**, 1295–1304 (2020).

6. Natali, A. *et al.* Insulin Sensitivity, Vascular Reactivity, and Clamp-Induced Vasodilatation in Essential Hypertension. *Circulation* **96**, 849–855 (1997).

7. Rocha, E. A. *et al.* Dysautonomia: a Forgotten Condition — Part 1. *Arq. Bras. Cardiol.* **116**, 814–835 (2020).

8. Bottino, D. A. & Bouskela, E. Non-invasive techniques to access in vivo the skin microcirculation in patients. *Front. Med.* **9**, 1–7 (2023).

9. Fedorovich, A. A., Korolev, A. I., Ososkov, V. S., Samatova, K. S. & Drapkina, O. M. New trends in non-invasive study of human skin microcirculation. *Cardiovasc. Ther. Prev.* **24**, 4412 (2025).

10. Mamontov, O. V., Shcherbinin, A. V., Romashko, R. V. & Kamshilin, A. A. Intraoperative imaging of cortical blood flow by camera-based photoplethysmography at green light. *Appl. Sci.* **10**, 6192 (2020).

11. Volkov, I. Y., Sagaidachnyi, A. A. & Fomin, A. V. Photoplethysmographic Imaging of Hemodynamics and Two-Dimensional Oximetry. *Opt. Spectrosc.* **130**, 452–469 (2022).

12. Kamshilin, A. A. *et al.* Accurate measurement of the pulse wave delay with imaging photoplethysmography. *Biomed. Opt. Express* **7**, 5138–5147 (2016).

13. van Duijvenboden, S. *et al.* Pulse Arrival Time and Pulse Interval as Accurate Markers to Detect Mechanical Alternans. *Ann. Biomed. Eng.* **47**, 1291–1299 (2019).

14. Finnegan, E. *et al.* Pulse arrival time as a surrogate of blood pressure. *Sci. Rep.* **11**, 22767 (2021).

15. Babchenko, A. *et al.* Increase in pulse transit time to the foot after epidural anaesthesia treatment. *Med. Biol. Eng. Comput.* **38**, 674–679 (2000).

16. Boutouyrie, P., Briet, M., Collin, C., Vermeersch, S. & Pannier, B. Assessment of pulse wave velocity. *Artery Res.* **3**, 3–8 (2009).

17. Sang, T., Lv, N., Dang, A., Cheng, N. & Zhang, W. Brachial-ankle pulse wave velocity and prognosis in patients with atherosclerotic cardiovascular disease: a systematic review and meta-analysis. *Hypertens. Res.* **44**, 1175–1185 (2021).

18. Mohammed, H. *et al.* Meta-Analysis of Pulse Transition Features in Non-Invasive Blood Pressure Estimation Systems: Bridging Physiology and Engineering Perspectives. *IEEE Trans. Biomed. Circuits Syst.* **17**, 1257–1281 (2023).

19. Milan, A. *et al.* Current assessment of pulse wave velocity: comprehensive review of validation studies. *J. Hypertens.* **37**, 1457–1557 (2019).

20. Lewis, T. The Blood Vessels of the Human Skin. *Br. Med. J.* **2**, 61–62 (1926).

21. Johnson, J. M. & Kellogg Jr., D. L. Local thermal control of the human cutaneous circulation. *J. Appl. Physiol.* **109**, 1229–1238 (2010).

22. Kamshilin, A. A. *et al.* Novel Method to Assess Endothelial Function via Monitoring of Perfusion Response to Local Heating by Imaging Photoplethysmography. *Sensors* **22**, 5727 (2022).

23. Podolyan, N. P. *et al.* Imaging photoplethysmography quantifies endothelial dysfunction in patients with risk factors for cardiovascular complications. *Biomed. Signal Process. Control* **86**, 105168 (2023).

24. Vasilieva, M. E. *et al.* Improvement of Microvascular Function in Patients with Morbid Obesity After Bariatric Surgery Revealed by Imaging Photoplethysmography. *Obes. Surg.* **35**, 1001–1008 (2025).

25. Kamshilin, A. A. *et al.* A new look at the essence of the imaging photoplethysmography. *Sci. Rep.* **5**, 10494 (2015).

26. de Haan, G. & van Leest, A. Improved motion robustness of remote-PPG by using the blood volume pulse signature. *Physiol. Meas.* **35**, 2878–2886 (2014).

27. Poh, M.-Z., McDuff, D. J. & Picard, R. W. Non-contact, automated cardiac pulse measurements using video imaging and blind source separation. *Opt. Express* **18**, 10762–10774 (2010).

28. Kearney, J. K., Thompson, W. B. & Boley, D. L. Optical flow estimation: An error analysis of gradient-based methods with local optimization. *IEEE Trans. Pattern Anal. Mach. Intell.* **PAMI-9**, 229–244 (1987).

29. Allen, J. Photoplethysmography and its application in clinical physiological measurement. *Physiol. Meas.* **28**, R1–R39 (2007).

30. Barcroft, H. & Edholm, O. G. The effect of temperature on blood flow and deep temperature in the human forearm. *J. Physiol.* **102**, 5–20 (1943).

31. Taylor, W. F., Johnson, J. M., O'Leary, D. & Park, M. K. Effect of high local temperature on reflex cutaneous vasodilation. *J. Appl. Physiol.* **57**, 191–196 (1984).

32. Mizeva, I. A. & Vetrova, D. V. Pulsations of cutaneous blood flow during local heating. *Russ. J. Biomech.* **18**, 447–454 (2014).

33. Saumet, J. L., Abraham, P. & Jardel, A. Cutaneous Vasodilation Induced by Local Warming, Sodium Nitroprusside, and Bretylium Iontophoresis on the Hand. *Microvasc. Res.* **56**, 212–217 (1998).

34. Roberts, K. A. *et al.* Reproducibility of four frequently used local heating protocols to assess cutaneous microvascular function. *Microvasc. Res.* **112**, 65–71 (2017).

35. Stefanovska, A., Bracic, M. & Kvernmo, H. D. Wavelet analysis of

oscillations in the peripheral blood circulation measured by laser Doppler technique. *IEEE Trans. Biomed. Eng.* **46**, 1230–1239 (1999).

36. Mizeva, I. A., Podolyan, N. P., Mamontov, O. V., Sakovskaia, A. V. & Kamshilin, A. A. Study of 0.1-Hz vasomotion in microcirculation under local heating by means of imaging photoplethysmography. *Biomed. Signal Process. Control* **100**, 107188 (2025).

37. Carberry, P. A., Shepherd, A. M. M. & Johnson, J. M. Resting and maximal forearm skin blood flows are reduced in hypertension. *Hypertension* **20**, 349–355 (1992).

38. Mayrovitz, H. N. Effects of local forearm skin heating on skin properties. *Clin. Physiol. Funct. Imaging* **40**, 369–376 (2020).

39. Hsiu, H. *et al.* Connection between RR-interval length and the pulsatile microcirculatory flow. *Physiol. Meas.* **29**, 245 (2008).

40. Del Giorno, R., Troiani, C., Gabutti, S., Stefanelli, K. & Gabutti, L. Comparing oscillometric and tonometric methods to assess pulse wave velocity: a population-based study. *Ann. Med.* **53**, 1–16 (2021).

41. Poole, D. C. & Musch, T. I. Capillary-Mitochondrial Oxygen Transport in Muscle: Paradigm Shifts. *Function* **4**, zqad013 (2023).

42. Walløe, L. Arterio-venous anastomoses in the human skin and their role in temperature control. *Temperature* **3**, 92–103 (2016).

43. Bergersen, T. K. A search for arteriovenous anastomoses in human skin using ultrasound Doppler. *Acta Physiol. Scand.* **147**, 195–201 (1993).

44. Moghaddam, A. S., Reissig, L. F., Geyer, S. H. & Weninger, W. J. Arterio-venous Anastomoses of the Sucquet–Hoyer Type: Complexity and Distribution in the Human Dermis. *Microsc. Microanal.* **30**, 334–341 (2024).

45. Cao, M., Burton, T., Saiko, G. & Douplik, A. Remote Photoplethysmography with a High-Speed Camera Reveals Temporal and Amplitude Differences between Glabrous and Non-Glabrous Skin. *Sensors* **23**, 615 (2023).

46. Cui, W., Ostrander, L. E. & Lee, B. Y. In vivo reflectance of blood and tissue as a function of light wavelength. *IEEE Trans. Biomed. Eng.* **37**, 632–639 (1990).

47. Maeda, Y., Sekine, M. & Tamura, T. The advantages of wearable green reflected photoplethysmography. *J. Med. Syst.* **35**, 829–850 (2011).

48. Weinman, J., Hayat, A. & Raviv, G. Reflection photo-plethysmography of arterial-blood-volume pulses. *Med. Biol. Eng. Comput.* **15**, 22–31 (1977).

49. Anderson, R. R. & Parrish, J. A. The optics of human skin. *J. Invest. Dermatol.* **77**, 13–19 (1981).

50. Fung, Y. C., Zweifach, B. W. & Intaglietta, M. Elastic environment of the capillary bed. *Circ. Res.* **19**, 441–461 (1966).

51. *Human Physiology*. *Human Physiology* (Springer-Verlag, 1989). doi:10.1007/978-3-642-73831-9_20.

52. Chatterjee, S., Phillips, J. P. & Kyriacou, P. A. Monte Carlo investigation of the effect of blood volume and oxygen saturation on optical path in reflectance pulse oximetry. *Biomed. Phys. Eng. Express* **2**, 65018 (2016).